J Mol Model (2012) 18:4025–4032
DOI 10.1007/s00894-012-1402-7

ORIGINAL PAPER

"Russian doll" complexes of [*n*]cycloparaphenylenes: a theoretical study

Serguei Fomine · Mikhail G. Zolotukhin · Patricia Guadarrama

Received: 9 January 2012 / Accepted: 6 March 2012 / Published online: 30 March 2012

Abstract The formation of "Russian doll" complexes consisting of [*n*]cycloparaphenylenes was predicted using quantum chemistry tools. The electronic structures of multiple inclusion complexes containing up to four macrocycles were explored at the M06-2X/6-31G* level of theory. The binding energy between the macrocycles increases from the center to the periphery of the complex and can be >60 kcal mol^{-1} for macrocycles containing 14 and 19 repeating units. It has been demonstrated that additional electrostatic interactions originating from the asymmetric electron density distribution observed when comparing the concave and convex macrocycle sides are responsible for the high binding energies in these Russian doll complexes. Oxidation or reduction of the Russian doll complexes creates polarons that are delocalized across the complexes. In the case of polaron cations, most of the polarons are localized at the macrocycle with the smallest ionization potential; for polaron anions, the negative charge is localized across the outer rings of the complex. Because anion polarons are more delocalized than cation polarons, the relaxation energies of the polaron anions were found to be smaller than those of the polaron cations.

Keywords Macrocyclic compounds · DFT · Cycloparaphenylenes · Intermolecular interactions

Electronic supplementary material The online version of this article (doi:10.1007/s00894-012-1402-7) contains supplementary material, which is available to authorized users.

S. Fomine (✉) · M. G. Zolotukhin · P. Guadarrama
Instituto de Investigaciones en Materiales,
Universidad Nacional Autonoma de Mexico,
Apartado Postal 70-360, CU, Coyoacan,
04510, Mexico D.F., Mexico
e-mail: fomine@servidor.unam.mx

Introduction

Conjugated macrocycles have drawn much attention due to their unique electronic properties and capacity for self-assemby [1–10]. The properties of macrocycles differ from those of linear oligomers. For instance, it has been demonstrated that cyclooligothiophenes are able to form stable nanoaggregates due to π–π stacking interactions. These nanoaggregates show strong electron delocalization along their axes, similar to carbon nanotubes [11, 12]. It was also discovered that the most stable conformation of a cyclooligothiophene depends on the macrocycle size [13]. The unique architecture of a conjugated macrocycle allows the formation of host–guest complexes with a C60 molecule, which leads to the generation of materials with interesting electronic properties [14, 15].

Another family of conjugated cyclic molecules is the cyclooligonaphthalenes, which have recently been synthesized [10]. The members of this family possess very good charge carrier transport properties due to their ability to form columnar structures. These properties have enabled the successful fabrication of OLED devices based on cyclooligonaphthalenes. Yet another group of cyclic conjugated macrocycles is the cyclic oligofluorenes, which have also recently been prepared [16].

One of the simplest classes of conjugated macrocycles is the cycloparaphenylenes (CPPs) [17]. These molecules have recently received much attention due to their potential utilization in photoelectronic applications, since they represent the simplest single-walled armchair carbon nanotube possible. A novel synthetic approach to CPPs has allowed the preparation and characterization of a wide range of CPPs of different sizes, and the properties of these CPPs have been studied [18]. The spontaneous formation of triple onion type complexes based on nanorings and the C60 molecule has

also been reported [19]. Just like cyclic oligothiophenes, the properties of CCPs depend strongly on size and differ from those of linear oligomers.

If CPPs represent the simplest single-walled armchair carbon nanotube, what is the simplest multiwalled armchair carbon nanotube possible? The answer is multiple inclusion complexes of CPPs, also known as "Russian doll" complexes (Fig. 1). The unusual architecture of these complexes sets them apart from others formed by conjugated macrocycles, which yield columnar structures [11, 12].

Since multiwalled nanotubes are fairly stable, these complexes of CPPs should also be stable. Therefore, the aim of the research described in this paper was to predict the principal electronic properties of Russian doll complexes formed by CPPs using quantum chemistry tools.

Computational details

The modeling of intermolecular complexes in which dispersion interactions play an important role is a challenging task, requiring methods that take dynamic correlation into account. Wavefunction-based post-Hartree–Fock (HF) methods are inapplicable to such large systems; therefore, the only way to model intermolecular interactions in these complexes is density functional theory (DFT). The recently developed meta functional M06-2X was selected for this purpose [20], as it has been shown to perform very well for π–π stacking interactions between nucleic acid bases (it even outperforms the MP2 method), and the binding energies obtained with M06-2X are close to those obtained with the CCSD(T) method [21]. The M06-2X functional belongs to the fourth rung of Jacob's ladder, and incorporates electron spin density, density gradient, kinetic energy density, and HF exchange. This particular functional incorporates 54 % HF exchange. All calculations were carried out using the Gaussian 09 suite of programs [22].

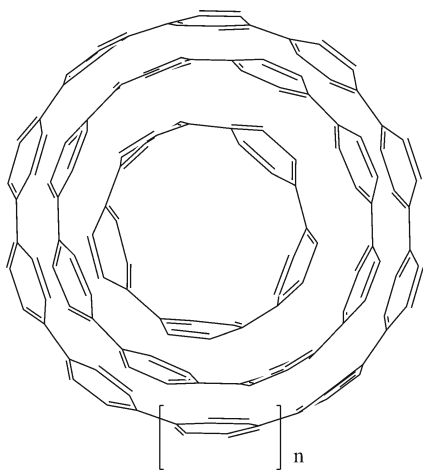

Fig. 1 An example of a triple inclusion Russian doll complex of CPP

Due to the limitations imposed by the large number of atoms in the systems under study, the medium-sized 6-31 G* basis set was used for the calculations. Since a relatively small size basis set was used for the calculations, no correction for basis set superposition error was performed, so the uncorrected binding energies were considered. Restricted and unrestricted formalisms were used for closed shell (neutral) and open shell systems (cation and anion radicals), respectively. No counterions were considered for charged molecules.

In the rest of this paper, Russian doll double, triple, and quadruple CPP complexes are denoted A-B, A-B-C, and A-B-C-D, respectively, where A, B, C and D are the number of repeating units in the CPP cycles involved in complex formation. Cation and anion radicals are referred to using superscript + and – symbols, respectively.

In its original form, DFT is only applicable to ground states. The Runge–Gross theorem extends the theory into the time domain, thus yielding time-dependent DFT (TD-DFT) and allowing the treatment of electronically excited states [23]. Currently, TD-DFT is the tool most widely applied to model electronic spectra [24]. The TD formulation of the M06-2X functional was used to model the excited states of Russian doll complexes.

Results and discussion

To characterize the Russian doll complexes, their binding energies, their adiabatic and vertical ionization potentials, their adiabatic and vertical electron affinities, and their S0→S1 and S0→S2 excitation energies were calculated, as well as the relaxation energies of the cation and anion radicals, respectively.

Neutral complexes

Binding energy

The principal characteristic of a complex is its binding energy. The binding energies of Russian doll complexes of CPPs are strongly dependent on the relative sizes of their components. The best fit between CPPs of different sizes in Russian doll complexes can be estimated from simple geometrical considerations. The distance between benzene rings in parallel displaced dimers is approximately 3.5 Å [25]. The average distance of 3.5 Å between the benzene rings in Russian doll complexes is achieved when the difference between the circumferences of two rings ($2\pi\Delta r$) is $2\pi\times$ 3.5 Å, where Δr=3.5 Å is the difference between the radii of two concentric rings. Therefore, in order to form the most

stable complex, the difference between the circumferences should be about 22 Å, which corresponds to an oligoparaphenylene containing five repeating units. This means that the successful formation of Russian doll complexes between CPPs requires two CPPs that differ by five repeating units. This rule is universal and does not depend on the ring size, since the difference between the circumferences of two rings depends only on Δr. If the difference between the inner and outer macrocycle is less than five benzene rings, the fit is too tight; if it is more than five, the average distance between the benzene rings of the inner and outer macrocycles is too large for effective interaction. Table 1 shows the calculated binding energies for Russian doll complexes containing two, three, and four CPPs. Note that this simple geometric rule works very well for different dimers.

It is worth noting that the estimates for the binding energy per repeating unit in the most stable CPP dimers (9–4, 14–9 and 19–14) are 7.05, 4.54, and 4.70 kcal mol^{-1}, which are much higher than the binding energy calculated for the parallel displaced benzene dimer at M06-2X/6-31 G* (3.15 kcal mol^{-1}).

It has been reported that in bowl-shaped polyarenes, the concave side has a more negative molecular electrostatic potential (MEP) than the convex side [26]. This is due to asymmetry in the π-electron density distribution between the two sides of polyarenes. Figure 2 shows the MEPs calculated for CPPs at the M06-2X/6-31 G* level of theory. The red color corresponds to a more negative MEP. In all cases, the concave side clearly has a more negative MEP than the convex one, with the largest difference seen for the smaller CPPs 4 and 9, due to the higher curvature of these CPPs. Therefore, apart from π–π stacking, which is mainly the result of dispersion forces, there are additional electrostatic attraction interactions between inner and outer macrocycles due to local dipole moments that point to the center of each macrocycle.

For CPP 4, the most stable complex is formed with macrocycle 9 (9–4). On the other hand, complex 8–4 has a negative binding energy, and complex 10–4 is less stable than 9–4. A similar situation holds for CPP 9; among the three complexes 13–9, 14–9, and 15–9, 14–9 is the most stable, with a binding energy of 40.9 kcal mol^{-1}. The most stable dimer formed by 14 as the inner macrocycle of a Russian doll complex is complex 19–14, which has a binding energy of 66.2 kcal mol^{-1}, while complexes 18–14 and 20–14 are less stable (Table 1). The inter-ring distances are similar for all three of the most stable dimers (9–4, 14–9, and 19–14), and lie in the range 3.2–3.6 Å. The binding energies, however, are quite different for these three dimers; they increase significantly from 28.2 to 66.2 kcal mol^{-1} with

Table 1 Binding energies (kcal mol^{-1}), adiabatic and vertical ionization potentials (IPa and IPv), adiabatic and vertical electron affinities (EAa and EAv), S0→S1 excitation energies of CPP complexes and individual macrocycles, and relaxation energies for cation (λ+) and anion radicals, (λ−), respectively (eV)

Macrocycles and complexes	Eb	IPa	IPv	λ+ [a]	EAa	EAv	λ− [b]	S0→S1
4	-	6.07	6.29	0.22	0.81	0.64	0.17	1.96
9	-	6.70	6.85	0.15	0.63	0.45	0.18	3.64
14	-	6.85	6.93	0.08	0.57	0.45	0.12	3.89
19	-	6.80	6.87	0.07	0.64	0.54	0.10	3.93
8-4	−24.3	-			-			-
9-4	28.2	5.51	5.74	0.23	0.82	0.66	0.16	1.90
10-4	22.9	-			-			-
13-9	29.0	-			-			-
14-9	40.9	6.29	6.40	0.11	0.66	0.56	0.10	3.38
15-9	33.3	-			-			-
18-14	−3.5	-			-			-
19-14	66.2	6.45	6.54	0.09	0.67	0.61	0.06	3.73
20-14	48.6	-			-			-
14-9-4	41.3; 28.5 [c]	5.29	5.60	0.31	0.79	0.60	0.19	1.99
19-14-9	68.3; 43.1 [d]	6.06	6.18	0.12	0.73	0.67	0.06	3.31
19-14-9-4	64.5;40.3;25.4 [e]	5.26	5.56	0.30	0.76	0.66	0.10	2.10

[a] $\lambda+ = IPv - IPa$

[b] $\lambda- = EAa - EAv$

[c] Binding energies between macrocycles 14 and 9 and between 9 and 4, respectively

[d] Binding energies between macrocycles 19 and 14 and between 14 and 9, respectively

[e] Binding energies between macrocycles 19 and 14, between 14 and 9 and between 9 and 4, respectively

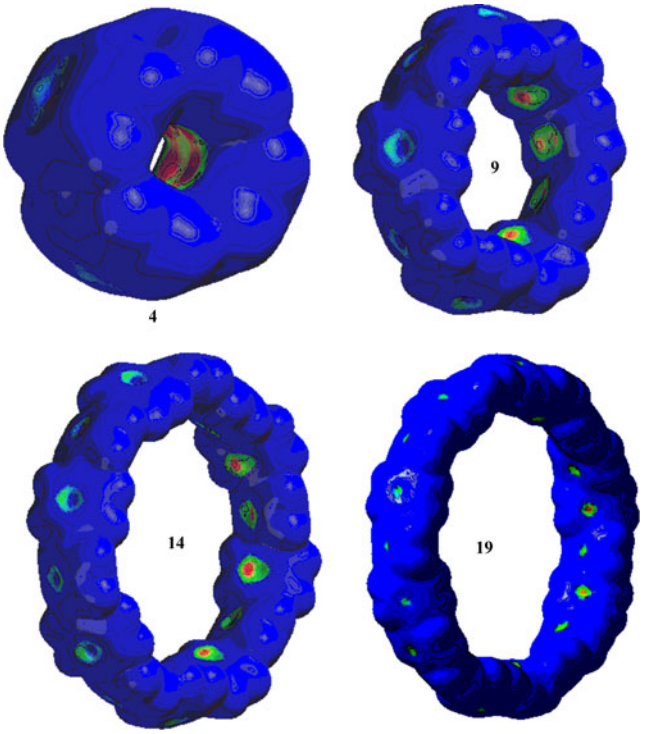

Fig. 2 Electrostatic potential mapped onto the total electron density surface of each CPP, calculated at the M06-2X/6-31G* level

macrocycle size in the following order: 9–4, 14–9, 19–14. This trend is easy to explain by invoking the increasing contact area between macrocycles with size, which in turn implies an increasing number of interacting π-orbitals. A similar situation was observed for the binding energies of acene dimers, where interaction energies increased almost linearly with the number of rings [27]. Therefore, the binding energy between concentric CPP macrocycles in Russian doll complexes increases from the center to the periphery of the complex.

Excited states

According to the literature [18], the gap between the HOMO and the LUMO decreases with the number of repeating units for linear oligoparaphenylenes, while it increases for CPPs. As we might have expected, this trend also holds for S0→S1 excitation energies of CPP oligomers (Table 1). As seen, the lowest estimated S0→S1 energy is obtained for macrocycle 4 (1.96 eV) and the highest for 19 (3.93 eV). When examining the S0→S1 energies for Russian doll complexes with different configurations, it is apparent that the S0→S1 excitation energy is close to that of the smallest cycle in the complex. Thus, for all complexes containing macrocycle 4 (9–4, 14-9-4, and 19-14-4), the calculated S0→S1 energy is close to 2 eV. For complexes where the smallest macrocycle is 9 or 14, the S0→S1 excitation energy is close to 3.3 and 3.8 eV, respectively. These facts suggest that, in spite of the rather high binding energies between individual CPPs in the Russian doll complexes, they behave as optically independent units, at least in the case of the S0→S1 transition, and electron excitation is limited to only one macrocycle. To corroborate this hypothesis, the dominant natural transition orbitals of Russian doll complexes for the S0→S1 transition were generated (Fig. 3) [28]. As seen from Fig. 3, the "hole" and the "particle"

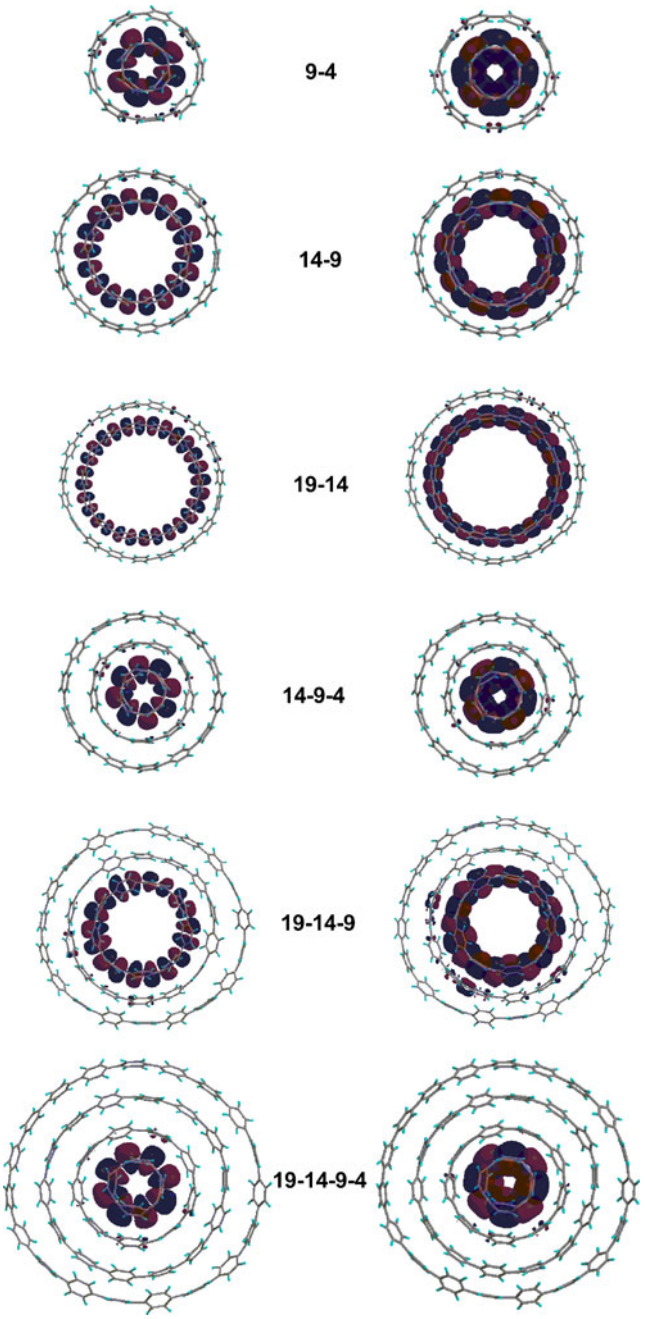

Fig. 3 The dominant natural transition orbital pairs for S0→S1 transitions in Russian doll complexes. The "hole" is on the *left*, the "particle" on the *right*

orbitals are always located on the same macrocycle (the smallest one) of the complex. Since this behavior could differ for higher excited states, a similar orbital analysis was also carried out for S0→S2 excitation, and the results are shown in Fig. 4. In this particular case, the electron transfer occurs from macrocycle 4 to 9 on excitation when both macrocycles are present in the complex. Otherwise, the situation is similar to the S0→S1 transition.

Light-harvesting properties

Due to their relatively small size, the electronic structures of Russian doll complexes can be explored at a relatively good theoretical level that sheds light on the electronic structures

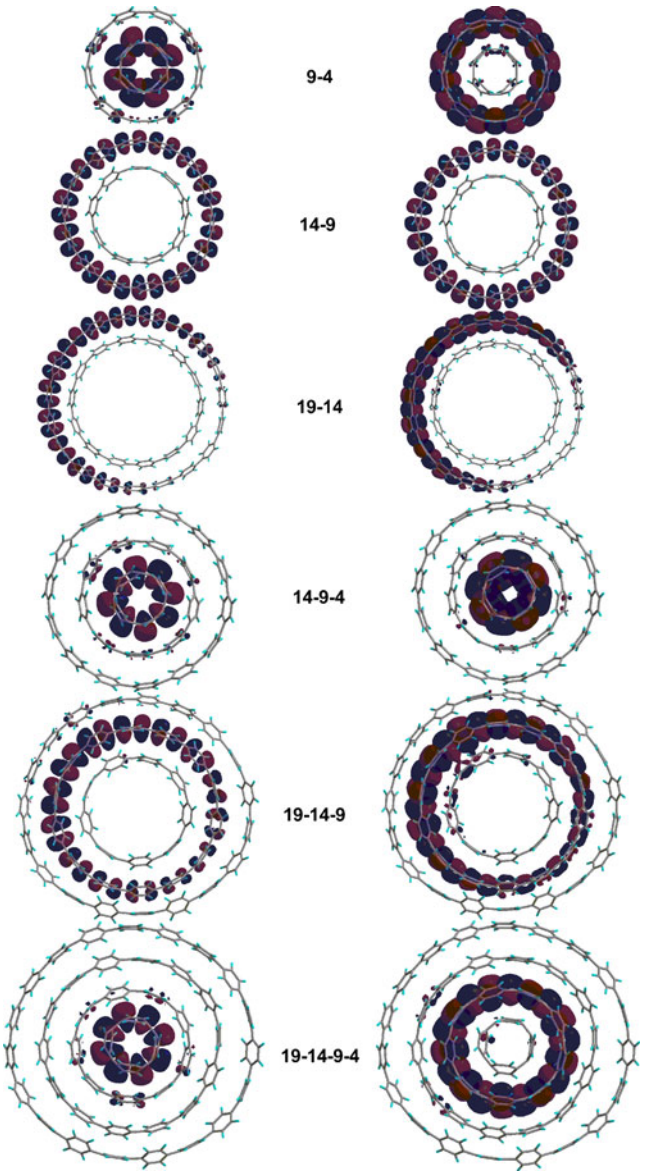

Fig. 4 The dominant natural transition orbital pairs for S0→S2 transitions in Russian doll complexes. The "hole" is on the *left*, the "particle" on the *right*

of multiwalled nanotubes. The unusual architecture of the Russian doll complexes formed from CPPs may provide them with unique electronic properties. Since the S0→S1 excitation energy increases from 4 to 19 (Table 1) and the macrocyles are optically independent, Russian doll complexes may therefore possess light-harvesting properties [29]. After the outer macrocycle of the complex absorbs light, exitons are generated that migrate through the inner rings of the molecular complex, carrying the energy obtained from the light. The exitons move to the smallest (central) ring in order to emit light. Because the energy of the light is captured and then transferred by exitons, the CPP Russian doll complex may act as an artificial molecular antenna. Unlike conventional dendrimeric molecular antennas, which are prepared by tedious multistep syntheses, the Russian doll complexes of CPP are likely to form by self-assembly of the macrocycles.

Cation radicals

It has been demonstrated that the HOMO–LUMO gap increases with the number of repeating units in CCPs, unlike linear oligomers [18]. This phenomenon results in an increase in redox potential with the number of repeating units for CCPs, while the opposite trend should be observed for linear oligomers. Single-electron oxidation or reduction of conjugated systems leads to the formation of delocalized cation or anion radicals, respectively (polaron cations or polaron anions). The oxidation or the reduction is accompanied by geometry relaxation, which leads to the localization of the charged defect. The geometry relaxation can be quantified as the relaxation energy (λ+ for cation radicals and λ− for anion radicals), which is the difference between the vertical and adiabatic ionization potentials (IPv, IPa) for polaron cations or between the respective electron affinities (EAv, EAa) in the case of one-electron reduction. It has been demonstrated that λ decreases with the length of the conjugated oligomer and that it is inversely related to polaron mobility [30].

Table 1 shows the IPs, EAs, and λ values of the CPPs and their corresponding complexes. As seen from Table 1, the IPs tend to increase with the size of macrocycle up to macrocycle 14. For macrocycle 19, a slight increase in the IP is observed. The relaxation energy decreases with macrocycle size in line with the data established for linear conjugated oligomers [30]. Two main trends in the IPs of Russian doll complexes can be observed. The first is that both the IPv and the IPa values of the complexes are always lower than the IP of the macrocycle with the lowest IP. For instance, the IPa of macrocycle 4 is 6.07 eV, while those for 9–4, 14-9-4, and 19-14-9-4 are 5.51, 5.29, and 5.26 eV. This behavior causes additional stabilization of positive charge by the electrons of other macrocycles involved in

complex formation. The second trend is a decrease in the IP of the complex with the number of macrocycles involved in complex formation, which is illustrated by the same example (a series of Russian doll complexes containing macrocycle 4). Just like the first trend, the second trend is related to the stabilization of positive charge by the electrons of additional macrocycles.

The charge distributions in cation and anion radicals can easily be visualized using the spin density distribution, since the charge of a polaron is always associated with an unpaired electron. Figure 5 shows the unpaired electron densities of cation and anion radicals of the Russian doll complexes. It is clear that most of the charge in a cation radical is always localized at the smallest inner macrocycle, since the IPs of the macrocycles increase with size. The only exception is the complex $(19–14)^+$. In this particular case, the IP of 19 is slightly lower than that of 14, but the positive charge is still localized at inner macrocycle 14. Since the difference between the IPs is very small (0.05 eV), this phenomenon can be explained by the better stabilization of the positive charge by the larger outer ring due to its increased delocalization.

Anion radicals

Due to the rather noticeable differences among the IPs of the CPPs, the delocalization of polaron cations in the Russian doll complexes can be successfully explained by the electronic properties of the individual macrocycles. This is not the case for anion radicals. The EAs of the CPPs are rather

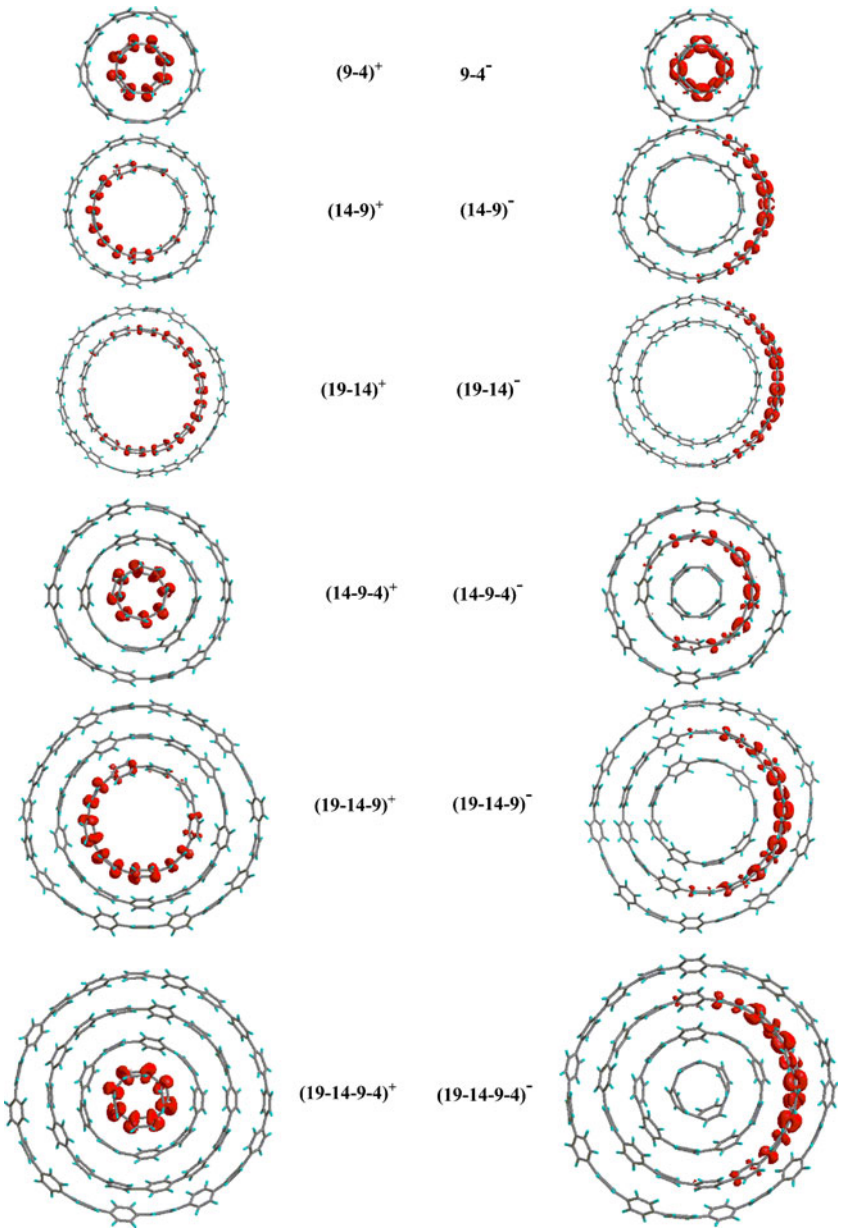

Fig. 5 Spin density distributions in cation and anion radicals of Russian doll complexes, estimated at the M06-2X/6-31Gd level

close. While the difference between the smallest and largest IPa is 0.73 eV, the difference between the smallest and largest EAs is much smaller (0.24 eV). As seen from Table 1, CPP 4 has the highest EAa (0.81 eV), while the EAs of other macrocycles are between 0.57 and 0.64 eV; therefore, the polaron anion macrocycle is not localized at the macrocycle with the highest EA. In the case of $(9–4)^-$, the polaron anion is located mostly at inner macrocycle 4 (0.87 e according to the Mulliken population analysis), in accordance with the relative EAs of the macrocycles. In all other cases, the delocalization of the polaron anion across large outer rings is observed to decrease electron repulsion. Thus, in the $(14–9)^-$ and $(19\text{-}14\text{-}9)^-$ anion radicals, 0.95–0.96 of the polaron anion is located at the outer macrocycles. In triple and quadruple Russian doll complexes, about 0.9 of the polaron anion is delocalized across the two largest rings, with about 0.7 localized over the penultimate macrocycle.

Relaxation energies

The relaxation energy is a function of polaron delocalization. Thus, when a polaron is localized at macrocycle 4 (maximal localization), λ is large. Thus, the largest λ+ values are seen for $(9–4)^+$, $(14\text{-}9\text{-}4)^+$, and $(19\text{-}14\text{-}9\text{-}4)^+$, where a polaron cation is delocalized across the smallest macrocycle. On the other hand, the smallest λ^+value was calculated for the most delocalized polaron cation $(19–14)^+$. As seen from Table 1, λ tends to increase with the size of the complex. This trend is similar to that observed for cyclo-oligothiophene aggregates, due to the increased deformabilities of large complexes [11, 12]. The relaxation energies for anion radicals (λ−) follow the same trend. Thus, one of the largest λ− values is seen for $(9–4)^-$, in which the polaron anion is located almost entirely at the inner macrocycle, where 0.89 of the extra electron is located, while the lowest λ− values were calculated for the $(19–14)^-$ and $(19\text{-}14\text{-}9)^-$ anions, where the anion radical is the most strongly delocalized. In all of the Russian doll complexes, the relaxation energies for polaron cations are higher than those for polaron anions due to the increased delocalization of polaron anions.

Conclusions

In this work, Russian doll complexes—a new type of intermolecular complex formed from CPPs—were predicted and their electronic properties were studied using quantum chemistry tools. The binding energy between macrocycles increases from the center to the periphery of each complex, due to the increase in the contact area between macrocycles with macrocycle size. The strongest binding was predicted to occur for CPPs that differ by five repeating units. The calculated absolute value of the binding energy reached 66 kcal mol^{-1} for large macrocycles, which is comparable with the strength of a chemical bond, due to additional electrostatic stabilization of the complex arising from the asymmetry of the electron density distribution between the concave and convex sides of the macrocycles. Since CPP units are optically independent in Russian doll complexes and the S0→S1 excitation energies increase with macrocycle size, the complexes have light-harvesting properties, because they transfer energy from the outer macrocycles to the central ring. Single-electron oxidation or reduction creates polaron cations or polaron anions that are delocalized across the complex. In cation radicals, most of the polaron is localized at the macrocycle with the smallest ionization potential, while the polaron is localized across the outer rings of the complex in anion radicals. Due to the increased delocalization in polaron anions compared to that in polaron cations, relaxation energies are smaller for the latter.

In conclusion, theoretical exploration of Russian doll CPP complexes—based on a combination of supramolecular, electrostatic, and van der Waals interactions—will provide access to novel nanostructures with size, shape, and electronic complementarity between the molecular components.

Acknowledgments The authors acknowledge financial support from the National Council for Science and Technology (CONACyT) of Mexico (grants 151277 and 151842) and the Head Office for Academic Personnel Affairs (DGAPA), as well as grant IN 104211 of the Program for the Assistance of Research and Innovation Projects (PAPIIT). The editorial assistance of Dr. E.S. Wilks is also appreciated.

References

1. Krömer J, Rios-Carreras I, Fuhrmann G, Musch C, Wunderlin M, Debaerdemaeker T, Mena-Osteritz E, Bäuerle P (2000) Angew Chem Int Ed 39:3481–3486
2. Mena-Osteritz E, Bäuerle P (2001) Adv Mater 13:243–246
3. Bong DT, Clark TD, Granja JR, Ghadiri MR (2001) Angew Chem Int Ed 40:988–1011
4. Mena-Osteritz E (2002) Adv Mater 14:609–616
5. Fuhrmann G, Debaerdemaekerb T, Bäuerle P (2003) Chem Commun 948–949
6. Bednarz M, Reineker P, Mena-Osteritz E, B uerle P (2004) J Luminescence 110:225–231
7. Ryu J-H, Oh N-K, Lee M, (2005) Chem Commun 1770–1772
8. Kawase T, Kurata H (2006) Chem Rev 106:5250–5273
9. Nakao K, Nishimura M, Tamachi T, Kuwatani Y, Miyasaka H, Nishinaga T, Iyoda M (2006) J Am Chem Soc 128:16740–16747
10. Nakanishi W, Yoshioka T, Taka H, Xue JY, Kita H, Isobe H (2011) Angew Chem Int Ed 50:5323–5326
11. Garcia M, Ramos E, Guadarrama P, Fomine S (2009) J Phys Chem A 113:2953–2960
12. Flores P, Guadarrama P, Ramos E, Fomine S (2008) Phys Chem A 112:3996–4003
13. Zade SS, Bendikov M (2006) J Org Chem 71:2972–2981
14. Mena-Osteritz E, Bäuerle P (2006) Adv Mater 18:447–451
15. Garcia M, Guadarrama P, Fomine S (2010) J Phys Chem A 114:5406–5413
16. Simon SC, Schmaltz B, Rouhanipour A, R der HJ, Müllen K (2009) Adv Mater 21:83–85

17. Schröder A, Mekelburger H-B, Vögtle F (1994) Top Curr Chem 17:2179–201
18. Iwamoto T, Watanabe Y, Sakamoto Y, Suzuki T, Yamago S (2011) J Am Chem Soc 133:8354–8361
19. Kawase T, Tanaka K, Shiono N, Seirai Y, Oda M (2004) Angew Chem Int Ed 43:1722–1724
20. Zhao Y, Truhlar DG (2008) Theor Chem Acc 120:215–241
21. Gu J, Wang J, Leszczynski J, Xie Y, Schaefer HF III (2008) Chem Phys Lett 459:164–166
22. Frisch MJ et al (2010) Gaussian 09 revision B.01. Gaussian Inc., Wallingford
23. Runge E, Gross EKU (1984) Phys Rev Lett 52:997–1000
24. Perdew JP, Ruzsinsky A, Tao J, Staroverov VN, Scuseria GE, Csonka GI (2005) J Chem Phys 123:062201
25. Hobza P, Selzle HL, Schlag EW (1996) J Phys Chem 100:18790–18794
26. Klärner FG, Panitzky J, Preda D, Scott LT (2000) J Mol Model 6:318–327
27. Gonzalez C, Lim EC (2003) J Phys Chem A 107:10105–10110
28. Martin RL (2003) J Chem Phys 118:4775–4777
29. Harigaya K (1999) Chem Phys Lett 300:33–36
30. Zade SS, Bendikov M (2008) Chem Eur J 14:6734–6741